

Layered Single-Metal Hydroxide/Ethylene Glycol as a New Class of Hybrid Material

Asayo Kasai and Shinobu Fujihara*

Department of Applied Chemistry, Faculty of Science and Technology,
Keio University, 3-14-1 Hiyoshi, Kohoku-ku, Yokohama 223-8522, Japan

Received September 8, 2005

Neutral ethylene glycol (EG) molecules have been intercalated into zinc hydroxide layers to produce a new hybrid material in which only one kind of metal ion is included. Initially, layered basic zinc acetate (LBZA, $Zn_5(OH)_8(CH_3COO)_2 \cdot 2H_2O$) was prepared from a methanolic zinc acetate dihydrate solution. The immersion of LBZA in EG resulted in its intercalation, which was accompanied by an interlayer expansion of 7.12 Å, as revealed by X-ray diffractometry. A Fourier transform infrared spectroscopic study indicated that the new compound contained both the acetate groups and the EG molecules. Together with thermogravimetry-differential thermal analysis, a composition of the new compound was estimated to be $Zn_5(OH)_8(CH_3COO)_2(HOC_2H_4OH)_2 \cdot 2H_2O$. The EG intercalation was found to increase the dehydration temperature of the zinc hydroxide layers from 130 to 180 °C. So the thermally stable material is then promising as a new class of precursors in creating organic–inorganic nanocomposites.

Introduction

A family of compounds known as “layered double hydroxides” (LDHs) consists of positively charged metal hydroxide layers with anions and water molecules existing between them.¹ LDHs have a general formula of $[M^{2+}_{1-x}M'^{3+}_x(OH)_2][A^{m-}]_{z/m} \cdot nH_2O$ where M^{2+} and M'^{3+} represent different kinds of divalent and trivalent metal ions in the octahedral sites of hydroxide layers and A^{m-} represents interlayered anions. Many works, so far, have reported to employ these compounds as materials for anion-exchange,² intercalation,^{3,4} delamination,⁵ catalysis,⁶ and a two-dimensionally confined reaction space caused by the lamella

structure.^{4,7} LDHs are also promising for fabricating organic–inorganic nanocomposite materials through the intercalation of organic compounds or delamination in organic polymers.¹

Inorganic components of nanocomposites should have certain kinds of useful electronic or optical functions such as electrical conduction, magnetization, and luminescence. In this sense, binary 3d transition metal compounds such as ZnO, CuO, NiO, Co_3O_4 , and Fe_3O_4 are of fundamental significance in designing and tailoring functional nanocomposites. However, because LDHs basically contain at least two different metal ions, they cannot be used in fabricating desirable nanocomposites of this kind.

Recently, we have succeeded in synthesizing “layered single-metal hydroxides” (LSHs) and controlling their crystal growth in chemical solutions.⁸ The LSHs have a general formula of $M(OH)_x(CH_3COO)_y \cdot nH_2O$ ($M = Co, Ni, \text{ or } Zn$); they are also called layered basic metal acetates.⁹ In this report, we have paid particular attention to layered basic zinc acetate (LBZA, $Zn_5(OH)_8(CH_3COO)_2 \cdot 2H_2O$) because its

* To whom correspondence should be addressed. E-mail: shinobu@applc.keio.ac.jp. Phone: +81 (0)45-566-1581. Fax: +81 (0)45-566-1551.

(1) (a) Leroux, F.; Besse, J. P. *Chem. Mater.* **2001**, *13*, 3507. (b) Rives, V., Ed. *Layered Double Hydroxides: Present and Future*; Nova Science Publishers: New York, 2001. (c) Giese, R. F., van Oss, C. J., Eds. *Colloid and Surface Properties of Clays and Related Materials*; Marcel Dekker: New York, 2002. (d) Auerbach, S. M., Carrado, K. A., Dutta, P. K., Eds. *Handbook of Layered Materials*; Marcel Dekker: New York, 2004. (e) Duan, X., Evans, D. G., Eds. *Layered Double Hydroxides: Structure and Bonding*, Vol. 119; Springer: Berlin, 2005.

(2) Rey, S.; Merida-Robles, J.; Han, K. S.; Guerlou-Demourgues, L.; Delmas, C.; Duguet, E. *Polym. Int.* **1999**, *48*, 277.

(3) Rives, V.; Ulibarri, M. A. *Coord. Chem. Rev.* **1999**, *181*, 61.

(4) Ogawa, M.; Kuroda, K. *Chem. Rev.* **1995**, *95*, 399.

(5) (a) Chen, W.; Feng, L.; Qu, B. J. *Chem. Mater.* **2004**, *16*, 368. (b) Chen, W.; Qu, B. *Chem. Mater.* **2003**, *15*, 3208. (c) Leroux, F.; Adachi-Pagano, M.; Intissar, M.; Chauviere, S.; Forano, C.; Besse, J. P. *J. Mater. Chem.* **2001**, *11*, 105.

(6) (a) Velu, S.; Suzuki, K.; Okazaki, M.; Kapoor, M. P.; Osaki, T.; Ohashi, F. *J. Catal.* **2000**, *194*, 373. (b) Nakagaki, S.; Halma, M.; Bail, A.; Arizaga, G. G. C.; Wypych, F. *J. Colloid Interface Sci.* **2005**, *281*, 417.

(7) Rhee, S. W.; Lee, J. H.; Jung, D. Y. *J. Colloid Interface Sci.* **2002**, *245*, 349.

(8) Hosono, E.; Fujihara, S.; Kimura, T.; Imai, H. *J. Colloid Interface Sci.* **2004**, *272*, 391.

(9) Fujihara, S.; Hosono, E.; Kimura, T. *J. Sol-Gel Sci. Technol.* **2004**, *31*, 165.

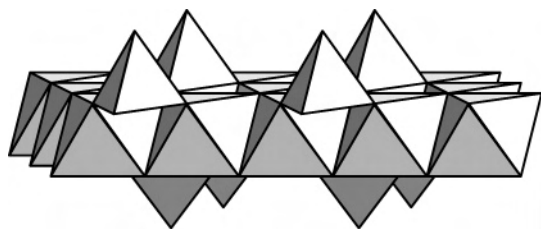


Figure 1. Structure of the zinc hydroxide layer present in LBZA.

decomposed form, ZnO, is a *n*-type wide-gap semiconductor. The structure of a zinc hydroxide layer in LBZA is a disordered lattice consisting of a main layer containing Zn^{2+} ions in octahedral coordination and disordered intermediate layers of tetrahedrally coordinated Zn^{2+} (Figure 1). As a result, the thickness and interspacing of the hydroxide layers of LBZA are larger than those of LDHs, thereby providing great potential for intercalating other organic compounds. This interesting structure can also be found in layered mixed metal hydroxyacetates containing Zn^{2+} in the tetrahedral sites and Ni^{2+} in the octahedral holes.¹⁰

We describe herein the successful intercalation of ethylene glycol (EG) molecules between the zinc hydroxide layers in LBZA. The parent LBZA was prepared as a mosaic-structured film on a glass substrate by chemical bath deposition (CBD) in a simple methanol solution of zinc acetate dihydrate, as reported previously.⁸ The LBZA films were simply immersed in EG at room temperature. Experimental results then provided the first example of the inclusion of neutral EG molecules into the layered single-metal hydroxide.

Experimental Section

Synthetic Procedures. A solution of LBZA for the CBD process was prepared by dissolving zinc acetate dihydrate ($\text{Zn}(\text{CH}_3\text{COO})_2 \cdot 2\text{H}_2\text{O}$, 99.9% metal purity) in anhydrous methanol by ultrasonating for 15 min. The concentration of zinc was fixed to 0.3 mol/dm³. Quartz glass slides of 1 mm in thickness were used as substrates for the deposition. The substrate was cleaned by sonicating in a dilute NaOH aqueous solution and then in high-purity acetone for 10 min each prior to use.

In the CBD procedure, the substrate was placed in bottles slantwise, which were filled with the solution and sealed up. The bottles were then kept still at 60 °C in a drying oven for 24 h. The LBZA films could be grown on both surfaces of the substrate and even on the bottle wall. The film on the substrate surface facing the bottom of the bottle grew only through the heterogeneous nucleation.⁸ On the other hand, the film grown on the opposite surface was composed not only of precipitates that were formed on the substrate but also of fallen particles originating from the homogeneous nucleation in the bulk of the solution.¹¹ As a result, the latter film was thicker and denser than the former. In any case, the films covered the substrate surface uniformly. We used the latter film in the present work to examine the EG intercalation described hereafter.

After deposition, the resultant LBZA films were rinsed with ethanol and dried at room temperature. The LBZA films were then

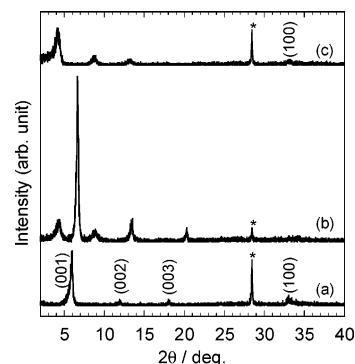


Figure 2. XRD patterns of (a) the as-deposited LBZA, (b) the LBZA–EG24, and (c) the LBZA–EG48 film. A peak labeled (*) represents silicon (111) added as an internal standard in the measurement.

put into bottles filled with EG and kept for 24 or 48 h at room temperature. Excessive EG was rinsed out of the films using ethanol after completion of the intercalation procedure.

Characterization. The crystal structure of the films was identified by X-ray diffraction (XRD) analysis with a Rigaku RAD-C diffractometer using Cu K α radiation. To examine the layered structure of the films correctly, the θ – 2θ scan was started from a low diffraction angle of $2\theta = 2^\circ$, using silicon powder, which was sprinkled on the films, as an internal standard in the measurement. It should be noted that the θ – 2θ scan of the films detects only crystallographic planes of crystallites parallel to the glass substrate surface. The organic species present in the films were examined by Fourier transform infrared (FTIR) spectroscopy with a BIO-RAD FTS-165 spectrometer using the KBr method. The thermal behavior of the films with and without EG intercalation was examined by thermogravimetry-differential thermal analysis (TG-DTA) with a Mac Science 2020S analyzer using a heating rate of 5 °C/min in flowing air. For the FTIR and the TG-DTA measurements, the films were removed from the substrate by scratching and were treated as powdery samples.

Results

XRD. The crystal structure of LBZA has been reported to be similar to that of layered basic zinc nitrate ($\text{Zn}_5(\text{OH})_8(\text{NO}_3)_2 \cdot 2\text{H}_2\text{O}$) and can be indexed in the hexagonal system according to XRD data.¹² Figure 2 shows XRD patterns of the parent LBZA film and the films immersed in EG for 24 (denoted as LBZA–EG24) and 48 h (LBZA–EG48). All the patterns are typical of the layered structure with strong peaks appearing in the lower 2θ range. The LBZA film exhibits three diffraction peaks at $2\theta = 6.01^\circ$ ($d = 14.72$ Å), 11.99° (7.37 Å), and 18.14° (4.87 Å), indexed as (001), (002), and (003), respectively.⁸ A peak at $2\theta = 33.06^\circ$ is attributed to (100). In the LBZA–EG24 film, additional peaks appear at $2\theta = 4.34^\circ$ (20.34 Å) and 8.80° (10.04 Å), indicative of the evolution of a new layered structure. Furthermore, the LBZA (001), (002), and (003) peaks increase in intensity and shift to a higher 2θ of 6.68° (13.22 Å), 13.43° (6.59 Å), and 20.29° (4.37 Å). In our previous report, we noted that the composition ratio of zinc, the hydroxyl group, the acetate group, and water could deviate from the stoichiometric value in accordance with the preparation conditions.⁸ The (001) interlamellar distance decreases

(10) (a) Yamanaka, S.; Ando, K.; Ohashi, M. *Mater. Res. Soc. Symp. Proc.* **1995**, 371, 131. (b) Rojas, R.; Barriga, C.; Ulibarri, M. A.; Malet, P.; Rives, V. *J. Mater. Chem.* **2002**, 12, 1071. (c) Rojas, R.; Barriga, C.; Ulibarri, M. A.; Rives, V. *J. Solid State Chem.* **2004**, 177, 3392.

(11) Hosono, E.; Fujihara, S.; Kimura, T. *Electrochim. Acta* **2004**, 49, 2287.

(12) (a) Stählin, W.; Oswald, H. R. *Acta Cryst. B* **1970**, 26, 860. (b) Poul, L.; Jouini, N.; Fiévet, F. *Chem. Mater.* **2000**, 12, 3123.

ed as the content of water or the acetate group was reduced. Therefore, a comparison of the (001) distance of the LBZA phase between the parent LBZA and the LBZA–EG24 film suggests the following. The parent LBZA film is composed of LBZA phases with slightly different compositions in terms of the intercalated species. After immersion in EG, the stoichiometry of the LBZA phases is considerably enhanced, thereby providing the increased (001) diffraction peak. We have confirmed the reproducibility of this result in repetitive experiments. The (001) distance of 13.22 Å observed for the LBZA phase in the LBZA–EG24 film is close to that of the stoichiometric LBZA prepared by a rapid titration method.¹³ A coherent shift of the peaks without peak broadening as a whole implies that the immersion of the LBZA film in EG promotes deintercalation of water molecules, taking account of the neutrality of the composition. This deintercalation seems to precede the intercalation of EG.

When the immersion time was increased to 48 h, the (001) peaks from the original LBZA could no longer be observed, thereby indicating the completed intercalation of the EG molecules. Instead, a new series of (001) peaks are observed at $2\theta = 4.34^\circ$ ($d = 20.34$ Å), 8.80° (10.04 Å), and 13.01° (6.79 Å). It should be noted that the peak position for the LBZA (100) diffraction remains unchanged after EG intercalation. As a result, a new layered compound, which has the same structure of the zinc hydroxide layer as LBZA and extended interlayer spacing of 20.34 Å, was successfully obtained.

A difference in the interlayer spacing between the LBZA phase ($d = 13.22$ Å) in the LBZA–EG24 film and the EG-intercalated film ($d = 20.34$ Å) corresponds approximately to the thickness of the intercalated EG layers. The observed thickness (7.12 Å) is comparable with that of “zigzag” double EG molecule layers intercalated in the clay mineral of vermiculite (6.8 Å).¹⁴ The slightly larger thickness of the present sample may be the result of additional species present in the interlayer, as discussed later.

FTIR. The presence of the EG molecules in the new compound was further examined by FTIR spectroscopy. Figure 3 compares the IR spectra of EG, the LBZA film, and the LBZA–EG48 film. At a higher wavenumber range, between 3700 and 3100 cm^{-1} , a broad absorption band is observed resulting from the stretching vibration modes of the hydroxyl group (–O–H) for all the samples. Vibrations of EG further result in intense absorptions at 2946 (C–H antisymmetric stretching) and 2879 cm^{-1} (C–H symmetric stretching). At a lower wavenumber range, EG displays absorption bands centered at 1085 and 1064 cm^{-1} (C–O stretching and C–O–H bending) and 882 and 864 cm^{-1} (CH_2 rocking vibration). The spectrum of LBZA has absorption bands from the –COO– group (1555 and 1440 cm^{-1}) and the – CH_3 group (1410, 1327, 1054, and 1015 cm^{-1}), thereby indicating the presence of the acetate (CH_3COO^-).

On the basis of these assignments, the spectrum of the LBZA–EG48 film can be interpreted as follows. The intense

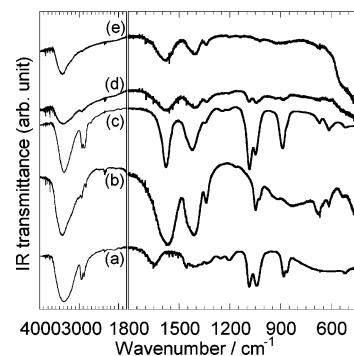


Figure 3. FT-IR spectra of (a) EG, (b) the as-deposited LBZA, and (c) the LBZA–EG48 film. Spectra of the LBZA–EG48 films heat-treated at (d) 100 and (e) 180 °C for 0.5 h are also shown.

absorption centered at 1555 and 1440 cm^{-1} indicates that the acetate remains definitely in the film. The bands around 1100–1000 cm^{-1} consist of contributions of both the – CH_3 group of the acetate (1054 and 1015 cm^{-1}) and the C–O/C–O–H groups of EG (1085 and 1064 cm^{-1}). The CH_2 rocking vibration of EG provides a better understanding of the spectrum. It was reported that the bands caused by the CH_2 rocking vibration shift to higher wavenumbers when EG is intercalated between inorganic layers. Actually, the original bands at 882 and 864 cm^{-1} were displaced to 900 and 868 cm^{-1} in boehmite and 919, 911, and 903 cm^{-1} in the Zn–Al– CO_3 LDH compound.^{15,16} This might be caused by the increase in bond order between two carbon atoms in the intercalated EG. In our LBZA–EG48 compound, the bands are shifted to a higher wavenumber of 890 cm^{-1} with a single broad absorption. Such an effect was reported for the EG-substituted lepidocrocite ($\text{FeO}(\text{OCH}_2\text{CH}_2\text{O})_{0.5}$) where the original two bands are overlapped as a result of the band shift.¹⁷ Together with the XRD result, these data result in the conclusion that EG was successfully intercalated between the zinc hydroxide layers.

It is known that EG can be absorbed in the clay layers in exchange for preexisting water molecules.¹⁸ In smectites solvated with EG, a basal spacing is expanded to approximately 17 Å, suggesting that a homogeneous EG bilayer is formed between the smectite layers.^{14,19} LDHs are also reported to be swelled by refluxing with EG. In this case, EG is bound to the host layers through the covalent bonding.^{15,16,20} However, the intercalation of EG into LSHs has never been reported so far.

TG-DTA. The thermal decomposition behavior of the LBZA and the LBZA–EG48 film was examined by the TG-DTA analysis performed in air. As shown in Figure 4, a gradual weight loss is observed at temperatures up to 130

(13) Morioka, H.; Tagaya, H.; Kadokawa, J. I.; Chiba, K. *J. Mater. Sci. Lett.* **1999**, *18*, 995.

(14) Brindley, G. W. *Clay Miner.* **1966**, *6*, 237.

(15) Inoue, M.; Kondo, Y.; Inui, T. *Inorg. Chem.* **1988**, *27*, 215.

(16) Guimarães, J. L.; Marangoni, R.; Ramos, L. P.; Wypych, F. *J. Colloid Interface Sci.* **2000**, *227*, 445.

(17) Kikkawa, S.; Kanamaru, F.; Koizumi, M. *Inorg. Chem.* **1980**, *19*, 259.

(18) (a) Tunney, J. J.; Detellier, C. *Clays Clay Miner.* **1994**, *42*, 473. (b)

Tunney, J. J.; Detellier, C. *Clays Clay Miner.* **1994**, *42*, 552.

(19) Sato, T.; Watanabe, T.; Otsuka, R. *Clays Clay Miner.* **1992**, *40*, 103.

(20) (a) Tunney, J. J.; Detellier, C. *Chem. Mater.* **1993**, *5*, 747. (b) Inoue,

M.; Kominami, H.; Kondo, Y.; Inui, T. *Chem. Mater.* **1997**, *9*, 1614.

(c) Wypych, F.; Schreiner, W. H.; Marangoni, R. *J. Colloid Interface Sci.* **2002**, *253*, 180.

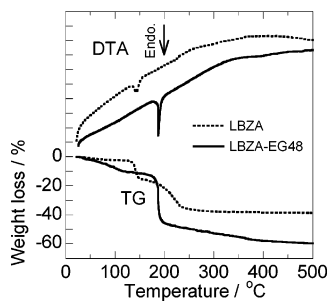


Figure 4. TG-DTA curves for the as-deposited LBZA and the LBZA-EG48 film.

°C for the LBZA film. This is attributed to the release of water intercalated into or adsorbed onto LBZA. An endothermic peak and a first-step large weight loss around 130 °C are the result of a dehydration decomposition reaction. It is known that zinc hydroxide undergoes a decomposition reaction to form ZnO in the temperature range 70–140 °C.²¹ This is also the case with LBZA, according to our previous study on the LBZA/ZnO transformation.⁸ In that study, we measured the enthalpy change, ΔH , to be +4.0 kJ/mol for the LBZA/ZnO transformation reaction. The endothermic nature of the reaction did not lead to the release of the acetate groups. Actually, higher temperatures were necessary to detach the acetate groups, as observed with a second-step weight loss at temperatures elevated to 230 °C. The absence of an exothermic peak is explained by the slow decomposition of the acetate groups or the direct departure of the acetate moiety.¹² From the TG curve, the approximate composition of LBZA was calculated as $\text{Zn}_5(\text{OH})_8(\text{CH}_3\text{COO})_2 \cdot 2\text{H}_2\text{O}$. As for the LBZA-EG48 film, the gradient of the TG curve in the low-temperature region is relatively steep, as compared to that for the LBZA, indicative of the presence of a larger amount of adsorbed water. An endothermic peak is then observed at a higher temperature of 180 °C with an abrupt weight loss. This indicates the simultaneous occurrence of dehydration and the departure of the acetate groups and EG. A plateau of the TG curve at temperatures higher than 180 °C is the final step of the transformation into zinc oxide by releasing EG. FTIR spectra of the LBZA-EG48 film heat treated at 100 or 180 °C for 0.5 h (Figure 3d and e) also shows evidence of the release of EG with or without the absorption at 1085 and 1064 cm^{-1} (C–O stretching and C–O–H bending).

Discussion

Our results strongly suggest that the final layered product (LBZA-EG48) has a structure where neutral EG is intercalated without replacing the other negatively charged components (CH_3COO^- and OH^-) of the parent LBZA. This is different from other structures often found in the EG-substituted layered compounds. For example, EG is covalently bonded to the metal hydroxide layers in boehmite, brucite, and LDHs.^{15,16,20} Because a certain amount of heat is usually necessary to form a covalent bonding, the works

previously reported were carried out by heating the compounds during the intercalation process. In contrast, the EG intercalation was achieved at room temperature in our method. Another important fact is that grafting of the inorganic layers with EG gives relatively small interlayer expansions, for example, 5.5 Å for boehmite and 3.52 Å for brucite.²⁰ In the present case, however, the observed expansion by the EG intercalation is as large as 7.12 Å. The “zigzag” double EG molecule layers intercalated in vermiculite (6.8 Å)¹⁴ are then conceivable structural units in our new layered compound, taking account of the presence of additional water layers.

As for the intercalation process at room temperature, the immersion of the parent LBZA film in EG once promotes deintercalation of water molecules, which precedes the intercalation of EG. If the acetate ions were deintercalated before the EG intercalation, the layered structure would be destroyed in the absence of the alternative negative OH^- in EG. This assumption is supported by the fact that zinc oxide is readily formed from zinc hydroxide in nonaqueous solvents such as methanol having relatively high dielectric constants (methanol: 32.6. EG: 37).²²

We have suggested, from the TG curve, that the LBZA-EG48 film contains the larger amount of adsorbed water. The weight loss from this excess amount of adsorbed water is estimated to be approximately 6% from a comparison between the parent LBZA and the LBZA-EG48 in the temperature range to 130 °C. A tentative composition of the new EG-intercalated compound can then be derived as $\text{Zn}_5(\text{OH})_8(\text{CH}_3\text{COO})_2(\text{HOC}_2\text{H}_4\text{OH})_2 \cdot 2\text{H}_2\text{O}$, assuming that the zinc hydroxide layers sustain their structure and taking into account of the molecular weight of each component and the weight loss (54%) observed in the thermal analysis. EG is known to be a relatively stable organic compound with a boiling point of 197.6 °C and an ignition point of 398 °C. The intercalation of EG therefore stabilizes the zinc hydroxide layers at temperatures up to 180 °C, as observed in the TG-DTA curve in Figure 4. The enhanced thermal stability of the layered structure is expected to be beneficial in fabricating functional nanocomposites including two-dimensional nanosheets.

Conclusions

The new EG-intercalated material was successfully derived from the layered basic zinc acetate. The XRD and FTIR analysis suggested the presence of the “zigzag” double EG molecule layers between the zinc hydroxide layers. The composition of the new compound was estimated to be $\text{Zn}_5(\text{OH})_8(\text{CH}_3\text{COO})_2(\text{HOC}_2\text{H}_4\text{OH})_2 \cdot 2\text{H}_2\text{O}$ according to the TG data. The EG intercalation increased the dehydration temperature of the zinc hydroxide layers from 130 to 180 °C. Such a thermally stable zinc hydroxide has not been reported so far. Our compound is promising as a precursor for new organic-inorganic nanocomposites.

IC051528D

(21) Oswald, H. R.; Asper, R. In *Preparation and Crystal Growth of Materials with Layered Structures*; Lieth, R. M. A., Ed.; D. Reidel: Dordrecht, The Netherlands, 1977.

(22) Hosono, E.; Fujihara, S.; Kimura, T.; Imai, H. *J. Sol-Gel Sci. Technol.* **2004**, *29*, 71.